Computers in Biology and Medicine 109 (2019) 22–32

Contents lists available at ScienceDirect

Computers in Biology and Medicine

journal homepage: www.elsevier.com/locate/compbiomed

Development and validation of a geometrically personalized finite element model of the lower ligamentous cervical spine for clinical applications

Mohammad Nikkhoo[a,*], Chih-Hsiu Cheng[b], Jaw-Lin Wang[c], Zahra Khoz[a], Marwan El-Rich[d], Nader Hebela[e], Kinda Khalaf[f]

[a] Department of Biomedical Engineering, Science and Research Branch, Islamic Azad University, Tehran, Iran
[b] School of Physical Therapy and Graduate Institute of Rehabilitation Science, Chang Gung University, Taoyuan, Taiwan, ROC
[c] Institute of Biomedical Engineering, College of Medicine and Engineering, National Taiwan University, Taipei, Taiwan, ROC
[d] Department of Mechanical Engineering, Khalifa University, Abu Dhabi, United Arab Emirates
[e] Orthopaedic Spine Surgery, Neurological Institute, Cleveland Clinic Abu Dhabi, Abu Dhabi, United Arab Emirates
[f] Department of Biomedical Engineering, Khalifa University of Science and Technology, Health Engineering Innovation Centre, Abu Dhabi, United Arab Emirates

ARTICLE INFO

Keywords:
Cervical spine
Biomechanics
Personalized modeling
Finite element analysis
Disc alteration

ABSTRACT

Epidemiological and clinical studies show that the magnitude and scope of cervical disease are on the rise, along with the world's rising aging population. From a biomechanical perspective, the cervical spine presents a wide inter-individual variability, where its motion patterns and load sharing strongly depend on the anatomy. This study aimed to first develop and validate a geometrically patient-specific model of the lower cervical spine for clinical applications, and secondly to use the model to investigate the spinal biomechanics associated with typical cervical disorders. Based on measurements of 30 parameters from X-ray radiographs, the 3D geometry of the vertebrae and intervertebral discs (IVDs) were developed, and detailed finite element models (FEMs) of the lower ligamentous cervical spine for 6 subjects were constructed and simulated. The models were then used for the investigation of different grades of IVD alteration. The multi directional range of motion (ROM) results were in alignment with the in-vitro and in-Silico studies confirming the validity of the model. Severe disc alteration (Grade 3) presented a significant decrease in the ROM and intradiscal pressure (flexion, extension, and axial rotation) on the C5-C6 and slightly increase on the adjacent levels. Maximum stress in Annulus Fibrosus (AF) and facet joint forces increased for Grade 3 for both altered and adjacent levels. The novel validated geometrically-personalized FEM presented in this study potentially offers the clinical community a valuable quantitative tool for the noninvasive analyses of the biomechanical alterations associated with cervical spine disease towards improved surgical planning and enhanced clinical outcomes.

1. Introduction

The sophisticated design of the cervical spine greatly contributes to its critical structural and functional roles in the human body. This includes acting as a shock absorber for the skull and brain, housing and protecting the brainstem, spinal cord, nerves and vessels, enabling forward-facing line of sight, and its biomechanical role in allowing for load transfer and providing wide complex physiological range of motion (ROM) [1]. This structural and functional complexity especially as it relates to multiplanar ROM, also makes the cervical spine particularly susceptible to injury. The magnitude and scope of cervical diseases, including disc degeneration, stenosis, and spondylolisthesis are on the rise, along with the world's growing aging population, and together with cervical trauma, they impose serious health and socioeconomic challenges on modern societies, globally [2].

In the past three decades, numerous theoretical, experimental (both in-vivo [3–5] and in-vitro [6–9]), as well as computational biomechanical studies [10–12] have been conducted in the hope of understanding the underlying mechanisms involved in cervical trauma and injuries. While some studies have been geared towards prevention of injuries, others deal with more effective diagnostic and treatment modalities [13]. Experimental clinical studies, using both in-vitro and in-vivo platforms, have the ability to provide relevant information regarding the biomechanical behavior and response of the cervical spine [14]. These studies are mostly limited by their inability to estimate the distributed stresses and strains within the structural components of the

* Corresponding author. Department of Biomedical Engineering, Science and Research Branch, Islamic Azad University, Daneshgah Blvd, Simon Bulivar Blvd, Sattari Highway, Tehran, 1477893855, Iran.
E-mail address: m.nikkhoo@srbiau.ac.ir (M. Nikkhoo).

https://doi.org/10.1016/j.compbiomed.2019.04.010
Received 14 March 2019; Received in revised form 14 April 2019; Accepted 14 April 2019

Table 1
Number of parameters to build the geometry of each vertebra. The characters in parentheses show the related parameters in Fig. 1.

Region	Number of Parameters
Vertebral Body	6 (A1-A6)
Articular Process	6 (B1-B6)
Spinous Process	6 (C1-C6)
Transverse Process and Foramen	5 (D1-D5)
Lateral mass and Lamina	3 (E1-E3)
Vertebral Foramen	2 (F1-F2)

spine. Finite element modeling (FEM) has hence emerged as a viable alternative due to its ability to more simply represent systems with complex loading and geometries and incorporate material non-linearities [15,16]. FEM also provide time- and cost-effective means to address various *what if* scenarios, thereby limiting the need for costly experimental animal and cadaveric studies [17].

On the other hand, despite the numerous published spinal FEMs in the last three decades, and the significant contribution of these models to the field of spinal biomechanics, their clinical applicability remains elusive. Issues ranging from anatomical/structural complexity of the spine and material properties' uncertainties [18,19], to loading parameter variability [20] and boundary conditions continue to plague the accuracy and reliability of FEM predictions, hence limiting the clinical applicability [17]. In addition to the inherent inter-individual variability limitation, the interface and ease with which the clinicians can update and implement the models also remain a challenge [21].

Current FEMs available in the literature are typically either exact models based on magnetic resonance (MRI) [22] and computed tomography (CT) [23–26], or idealized models based on simplified geometries and averaged approximated dimensions (so called parametric models) [27–33]. While exact models may be capable of representing subject-specific geometry, and are reliable for biomechanical studies, their clinical application is limited, as they constrained to input geometry, typically based on one or few subjects and typically time-consuming [21]. Parametric or idealized models, despite their simplifications, on the other hand may provide a viable alternative, as they are modular in design and can include patient-specific easily updated data using clinical images to account for the variability between specific individual subjects [29,31].

Few studies have investigated the influence of anatomical parameters on the biomechanical response of the cervical and lumbar spines [34]. Examples include studying the influence of cervical [31,35] and lumbar lordosis curvature [36], and scoliosis deformity [13] using FEM simulations. Most available models in the literature are obtained from CT or MRI. Despite the added accuracy provided by such models, they are plagued by several challenges as mentioned above, including the insensitivity to inter-subject variability, limited availability cost of MRI and CT scan images, as well as the added risk of radiation exposure in the case of CT scans.

The aim of this study was to develop and validate a robust, patient-specific FEM of the lower cervical spine viable for clinical applications. Our model uses a clinically driven user-friendly interface to automatically update the geometry for different patients using plain X-ray images. This work explores application of the model for the investigation of degenerative cervical spine disease as an example.

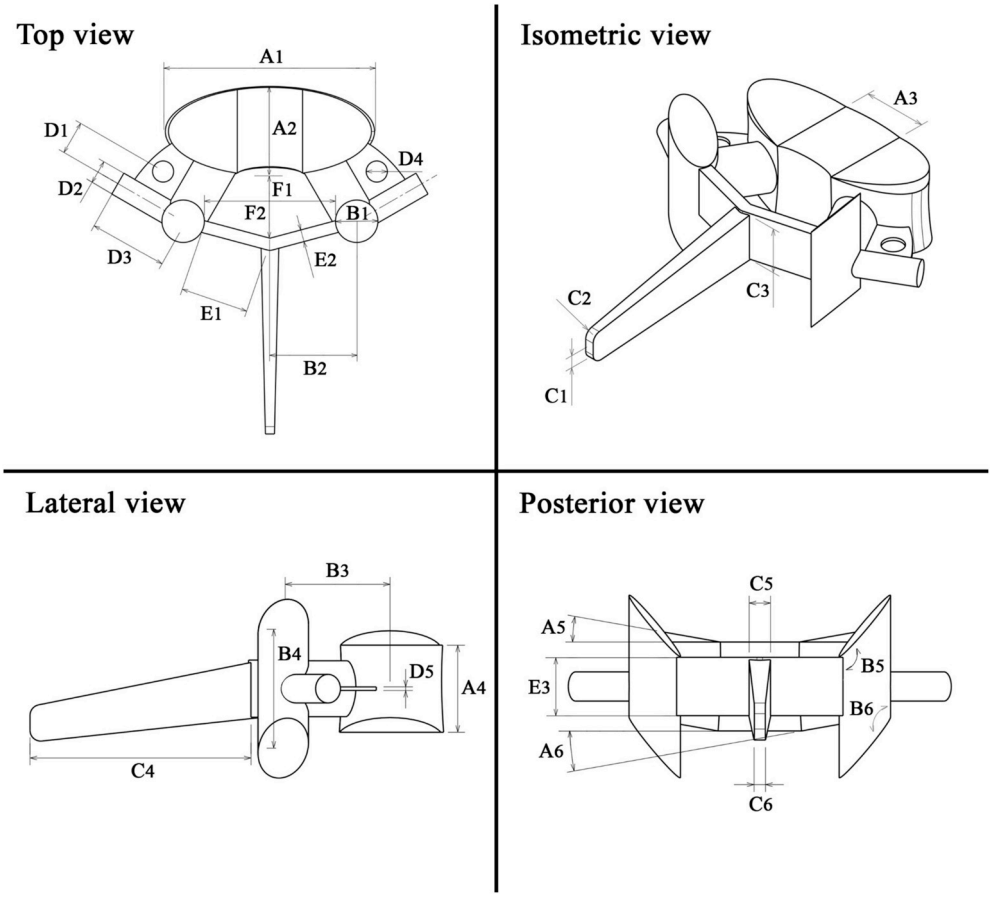

Fig. 1. Defined parameters for construction of the typical cervical vertebra.

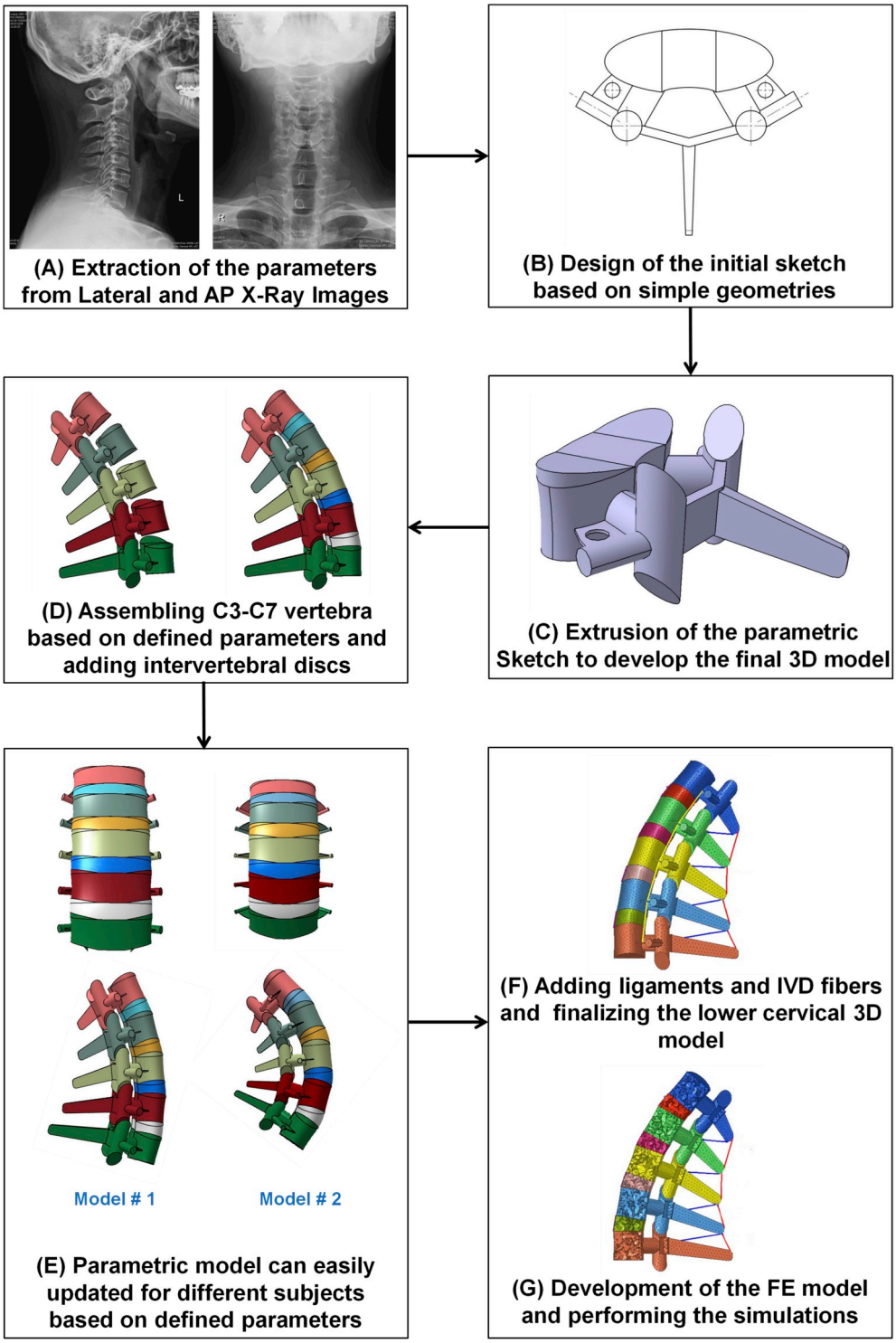

Fig. 2. Procedure of the parametric finite element modeling of the lower cervical spine.

2. Materials and methods

2.1. Parametric modeling of the geometry

2.1.1. Extraction of the anatomical parameters

The geometrical measures of the lower cervical vertebrae (C3–C7) of 6 subjects were selected from the data bank of our previous study (62 patients) [37]. The inclusion criteria for that study involved participants free of: (1) disc degeneration, spondylolisthesis, or any kind of cervical spine deformity (2) any history of surgery over the cervical, thoracic and/or lumbar spine. A signed informed consent had been obtained from all participants prior to their enrolment in the study, and the protocol was implemented in agreement with the Declaration of Helsinki (Oct 2013) and approved by the institutional ethics review committee at National Taiwan University Hospital and National Taiwan University College of Medicine. Lateral and AP radiographs of the cervical spine in neutral, flexion and extension perspectives in the standing position were captured under the supervision of a specialized radiologist. The images were imported to MATLAB image processing toolbox (Mathworks, Inc., Natick, MA, USA) for the measurement of the

Table 2
Material properties of the parametric finite element model.

Component	Mechanical Properties	Reference
Cortical Bone	E_{xx} = 11300 MPa, G_{xy} = 3800 MPa, υ_{xy} = 0.484 E_{yy} = 11300 MPa, G_{yz} = 5400 MPa, υ_{yz} = 0.203 E_{zz} = 22000 MPa, G_{xz} = 5400 MPa, υ_{xz} = 0.203	[40,41]
Cancellous Bone	E_{xx} = 140 MPa, G_{xy} = 48.3 MPa, υ_{xy} = 0.45 E_{yy} = 140 MPa, G_{yz} = 48.3 MPa, υ_{yz} = 0.315 E_{zz} = 200 MPa, G_{xz} = 48.3 MPa, υ_{xz} = 0.315	[40,41]
Annulus Fibrosus ground	Mooney–Rivlin Hyperelastic C1 = 0.56, C2 = 0.14, υ = 0.45	[40,41]
Nucleus Pulposus	Mooney–Rivlin Hyperelastic C1 = 0.12, C2 = 0.09, υ = 0.4999	[40,41]
Disc Fibers	Rebar elements, E = 500 MPa, υ = 0.3	[10]
Ligaments	Nonlinear Tension-only Truss (Fig. 3A and B)	[10,35,36]

Cross-section Area of the Ligaments (mm^2)

Level	ALL	PLL	LF	CL	ISL	SSL
C3-C5	11.1	11.3	46.0	42.2	13.0	9.0
C5-C7	12.1	14.7	48.9	49.5	13.4	9.0

*ALL: Anterior Longitudinal Ligament, PLL: Posterior Longitudinal Ligament, LF: Ligamentum Flavum, CL: Capsular Ligament, ISL: Interspinous Ligament, SSL: Supraspinous Ligament.

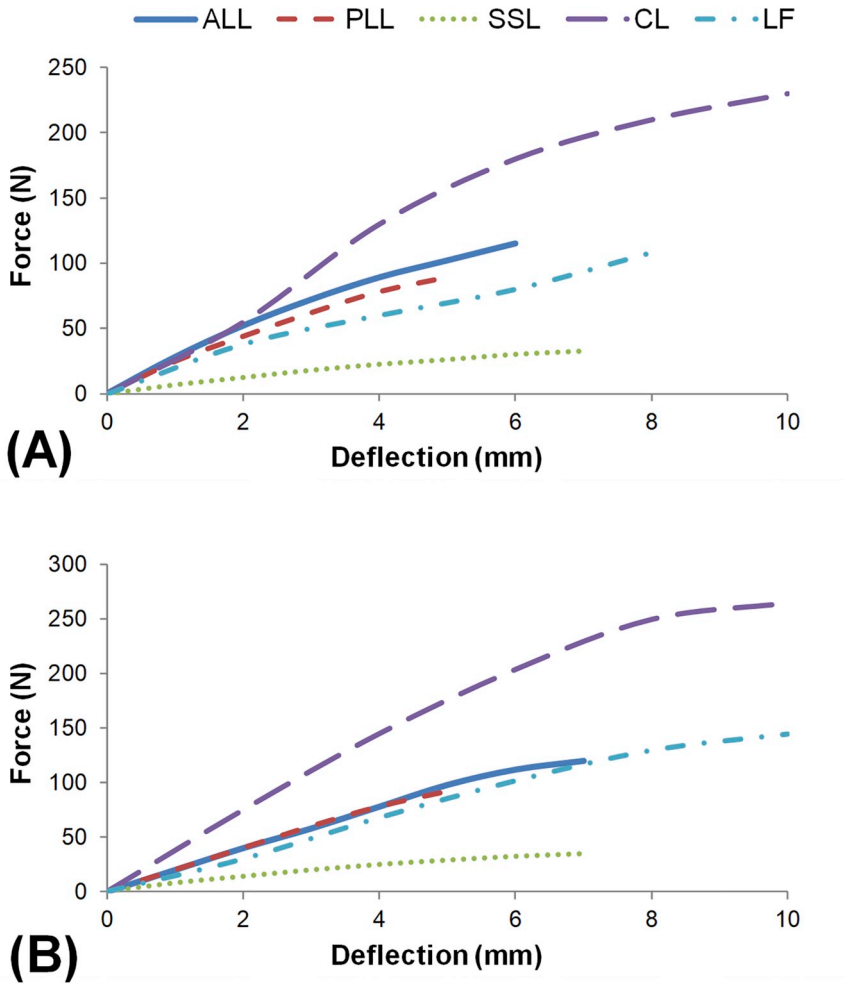

Fig. 3. Force-Deformation properties of the ligaments for (A) C3-C5 and (B) C5-C7 levels.

defined dimensions and angles. To ensure the reliability of the measurements, the process was repeated three times, and the average values were used in developing the model.

2.1.2. Construction of the parametric geometry

The geometry of the lower cervical spine (C3-C7) was developed based on the shape of a typical lower cervical vertebra and assembly

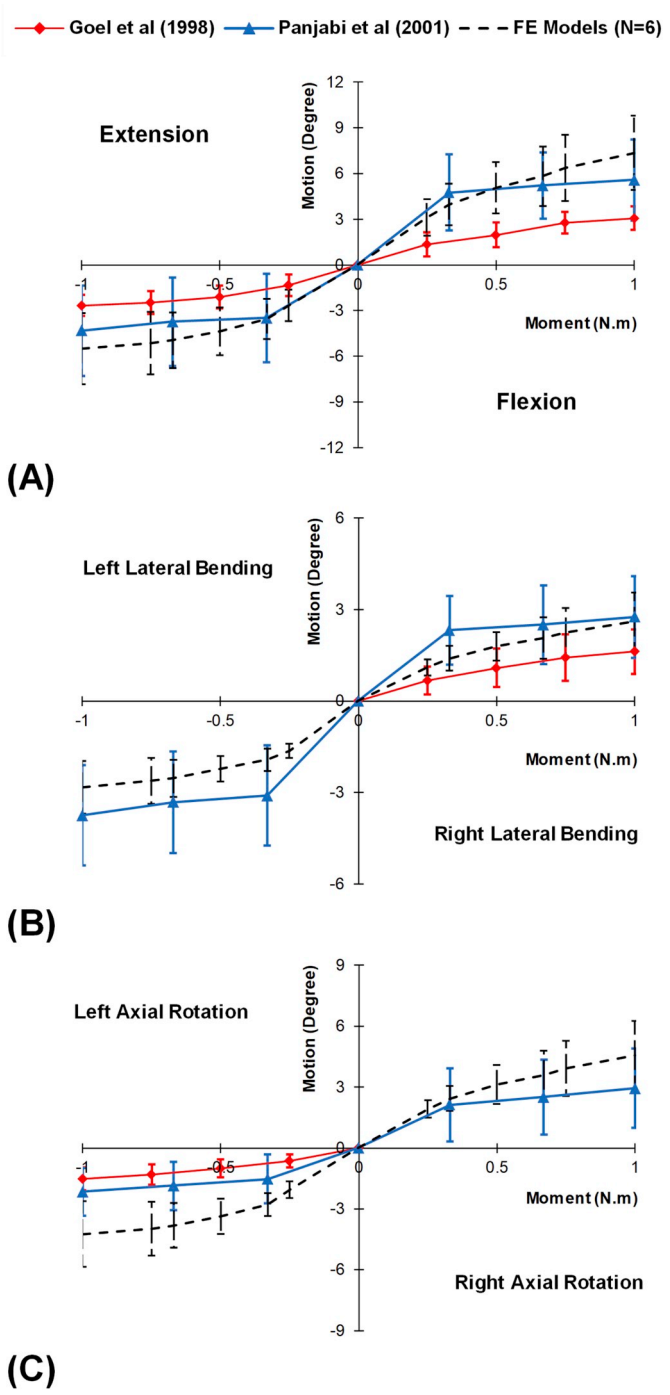

Fig. 4. Motion curves of C5-C6 for the average results of the 6 intact lower cervical models in (A) Flexion, (B) Extension, (C) Lateral Bending, and (D) Axial Rotation compared to the in-vitro experimental data [9] and FE results [48] in literature.

parameters. The typical vertebrae were constructed using simple geometries such as circles, ellipses, and cutting planes. A total of 28 parameters were marked on each vertebra on the lateral and AP images in neutral position to extract the vertebral geometric parameters (Table 1 and Fig. 1). Two extra parameters (i.e. the anterior height of the intervertebral disc (IVD) and the lordosis angle) were used to assemble five vertebrae and develop the final geometry (Fig. 2). Geometry of the IVD was built to fill the gap between the inferior surface of the upper vertebra and the superior surface of the lower vertebra (Fig. 2).

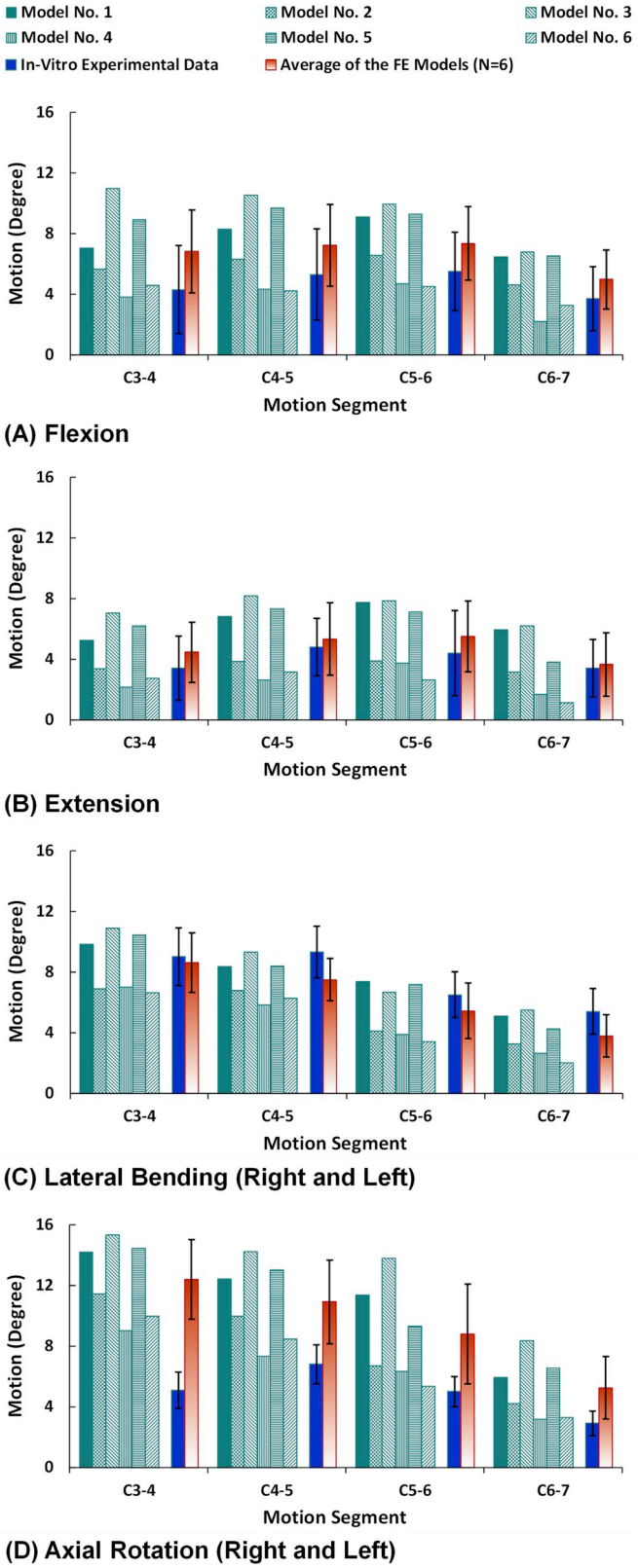

Fig. 5. Range of motions for the simulations of the 6 intact lower cervical models in (A) Flexion, (B) Extension, (C) Lateral Bending, and (D) Axial Rotation compared to the experimental results by Panjabi et al. [9].

Based on the defined geometrical constraints and relations, the geometrical model was designed to update automatically by entering new values of the independent parameters. As an example, Fig. 2E shows

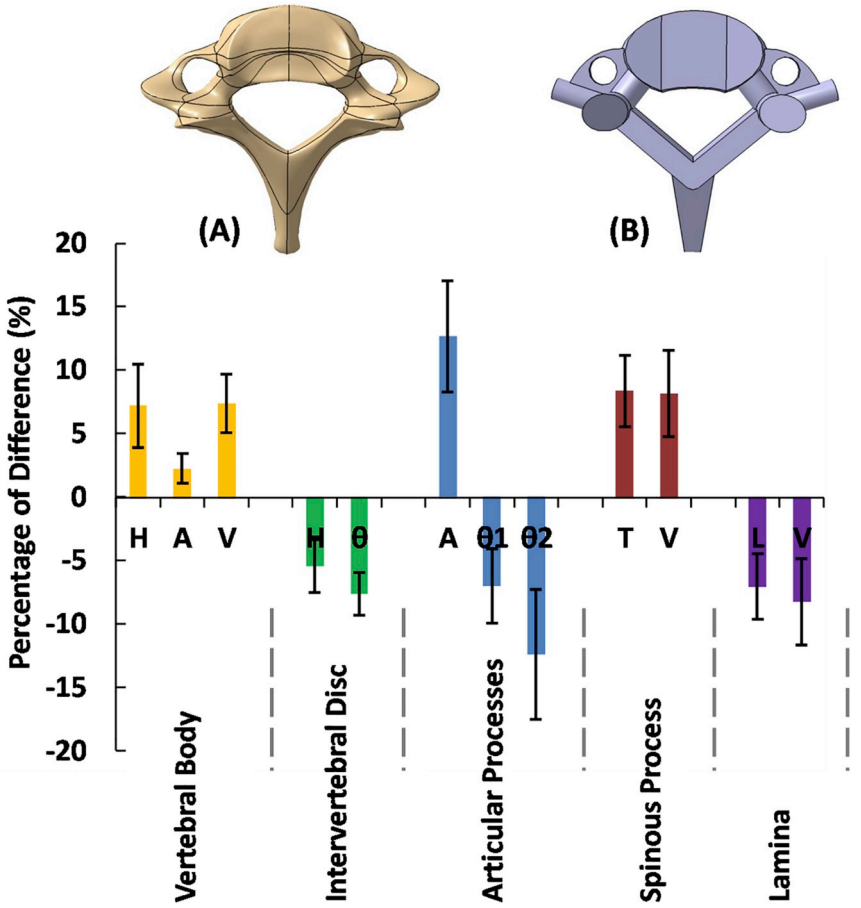

Fig. 6. The averaged geometry deviation for the main components of the C3-C7 cervical spine. C7 vertebra for (A) exact and the equivalent (B) parametric models is shown for comparison. Positive (+) and negative (−) values refer to the increase and decrease in the measured values of the parametric model as compared to the exact one. The aforementioned abbreviations are: H = Height, A = Area, V = Volume, θ = Angle, T = Thickness, and L = Length.

Table 3
Comparison of the calculated results for C5-C6 between the current parametric FE model and a previously developed exact FE model. The results are provided as the percentage of the difference.

	Flexion	Extension	Lateral Bending	Axial Rotation
ROM	+8.6%	−5.8%	−13.1%	+18.7%
IDP	+5.3%	−2.5%	−3.8%	+6.0%
Fiber Strain	+3.9%	−1.7%	−2.6%	+5.2%
Maximum Stress in AF	+11.4%	−8.1%	−7.7%	+15.8%
FJF	–	+29.5%	+24.3%	+32.2%

*ROM: Range of Motion, IDP: Intradiscal Pressure, FJF: Facet Joint Force.
**Positive (+) and negative (−) values refer to the increase and decrease in the calculated results of the parametric model as compared to the exact one.

two different updated models for subject No. 1 and No. 2, respectively, illustrating the capability of the model to easily incorporate and capture geometric differences.

2.2. FE modeling of healthy lower cervical spine

Based on measurements of 30 parameters extracted from the lateral and AP radiographs of each subject, the 3D geometry of the lower cervical spine was developed. Consequently, FE models of the lower cervical spine were developed for all 6 subjects including the typical vertebrae (C3-C7), IVDs, facet joints, and ligaments using Hypermesh (Hyperworks 12.0, Altair, USA) and ABAQUS (SIMULIA, Providence, RI, USA). In general, each lower cervical FE model consisted of 5 vertebrae, 4 IVDs (i.e., C3–C4, C4–C5, C5–C6, and C6–C7), 6 ligaments (i.e., anterior longitudinal ligament (ALL), posterior longitudinal ligament (PLL), ligamentum flavum (LF), capsular ligament (CL), interspinous ligament (ISL) and Supraspinous ligament (SSL)), as well as 4 pairs of facet joints. The IVDs were modeled as a composite material containing the nucleus pulposus (NP), annulus fibrosus (AF), ground substance, and collagen fibers. The fluid-like behavior of the NP and AF was simulated based on Mooney–Rivlin hyperelastic materials (Table 2). To consider the effect of the collagen fibers, rebar elements were embedded in the ground substance matrix in 6 layers, and were arranged in an alternating crisscross manner with 25-degree orientation [10]. The ligaments were modeled using nonlinear truss elements, which can be activated only in tension. They were then attached to bony structures at fixed points based on standard human anatomy. As the geometrical parameters were updated, the length of ligaments was automatically updated as well. Ligament material properties were defined using force-displacement curves [10,38,39] (Fig. 3), as well as the cross-sectional areas, from literature (Table 2). Mechanical properties of other components were assumed as linear elastic based on available data in literature (Table 2) [10,40–42]. The facet joints were modeled as an ellipse, in which the extruded cylinders were cut obliquely with a 3D oriented plane. A gap distance of 0.3 mm was chosen to simulate the articulation of facet joints [41], and surface to surface contact in both tangential and normal directions was considered in model. An exponential pressure over closure [40,43] was used to simulate normal contact rule, in addition to a tangential frictionless property. The geometry was meshed using the Hypermesh software (Hyperworks 12.0, Altair, USA) using 4-node tetrahedral solid elements. A quasi-static analysis was implemented for the computational algorithms, where the selected number of the elements and nodes were 52, 723, and 129, 908, respectively, based on meshing sensitivity analyses. To ensure

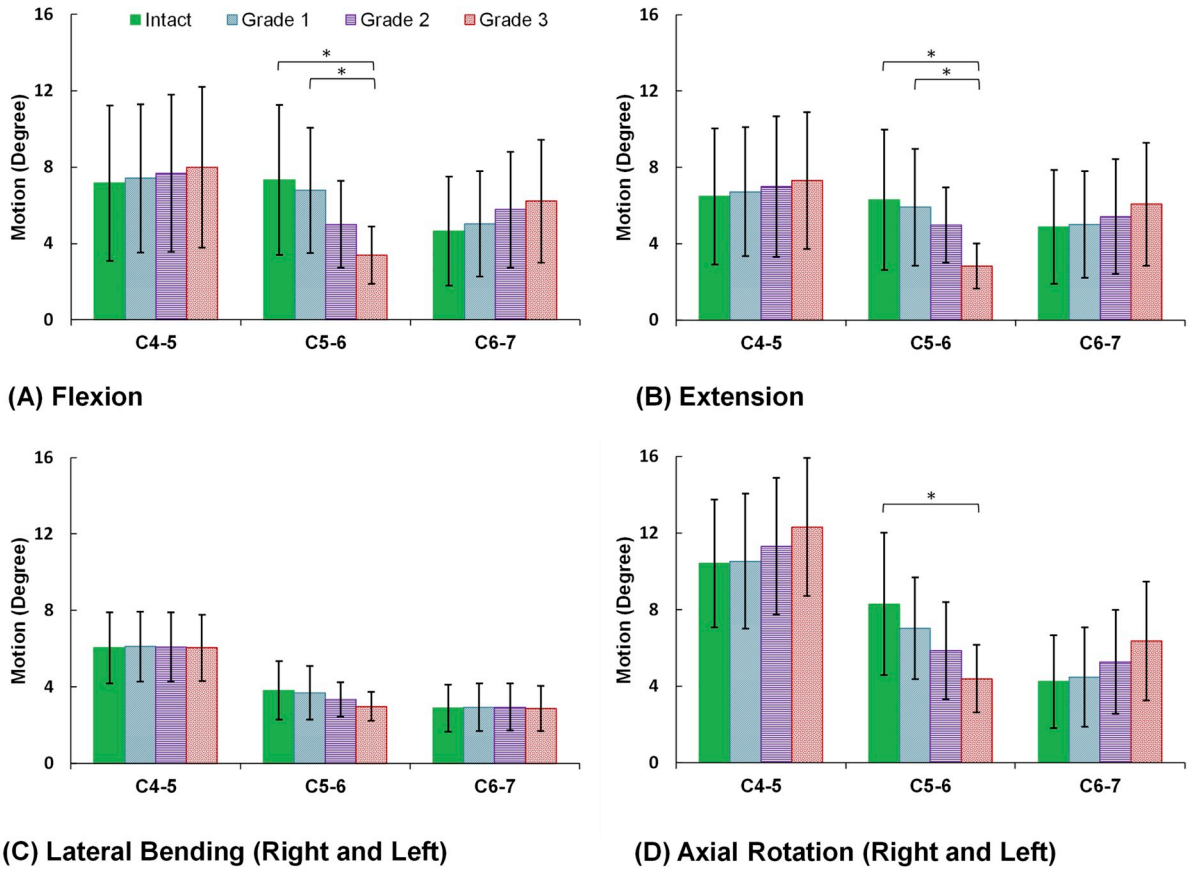

Fig. 7. Variation of the range of motion in C4-C5, C5-C6, and C6-C7 levels in simulated Intact and altered cervical spine (Grade 1 to 3). The error bars indicate the standard deviation and p value less than 0.05 was considered as significant difference and marked by "*".

convergence, the maximum moment was divided into five sub-steps, whereas each sub-step was iteratively determined using Newton's method.

To evaluate the validity of the intact model, a pure moment of 1 N m was applied at the superior surface of C3 in three different orientations: (1) flexion and extension, (2) right and left lateral bending, and (3) left and right axial rotation. The lowest vertebral surface was set to zero for all degrees of freedom representing a fixed surface reference for the model. The simulations were performed for all 6 subject-specific models with the same boundary conditions. The results of the intersegmental ROM were compared to experimental studies from literature [9]. To evaluate the level of confidence on the results obtained using simplified geometry, another model was developed based on measurements from our previous cervical FE model with exact geometry [23]. The ROM, intradiscal pressure (IDP), fiber strain, maximum stress in AF ground, and facet joint forces (FJF) were compared using the same geometry.

2.3. FE modeling of lower cervical spine with altered disc disease

Disc degeneration was selected as an example of a potential clinical application of our validated model. Three different grades of disc degeneration/alteration were simulated at the C5-C6 level. The disc heights were reduced by 25%, 50%, and 75%, respectively, to mimic the different clinical grades of disc alteration [44,45]. The NP compressibility was increased in the altered discs based on available data from literature [46]. The three cervical spine models with altered discs ($n = 6 \times 3$) were then simulated under a pure moment of 1 N m in different directions (i.e., Flexion, Extension, Lateral Bending, and Axial Rotation), under the boundary conditions previously presented, and following a 50 N preload to mimic the head weight [47]. The results were compared with those of the intact models ($n = 6$).

2.4. Statistical analyses

The simulation results of the ROMs, as well as the IDP, maximum stress in AF, and FJF in the altered IVDs and adjacent level IVDs were compared among intact and altered discs using one-way ANOVA tests. The differences were considered to be significant at a P value < 0.05.

3. Results

Automatic 3D geometry reconstruction was successfully performed directly upon inputting the measured parameters from the Lateral and AP radiographs. Mesh generation was updated based on the new geometry in less than 1 min. For all 6-updated FE models, the mesh sensitivity analyses were verified and the accuracy of the numerical calculations was confirmed. Nonlinear trends of motion were observed for all of the 6 subject-specific FEMs by increasing the moment. The calculated averaged intersegmental ROM curves for C5-C6 were compared with available in-vitro experimental data [9], as well as, FE results [48] from literature (Fig. 4). Furthermore, the calculated inter-segmental ROMs for all 6 intact subject-specific FE models and their averaged results were compared with in-vitro experimental data available in literature [9] in flexion and extension (Fig. 5A and B), lateral bending (Fig. 5C), and axial rotation (Fig. 5D). Anatomical differences of individual vertebrae for different subjects demonstrated variation of inter-segmental ROMs (Fig. 5). The analysis of the geometrical deviation between the exact and parametric models showed that the average

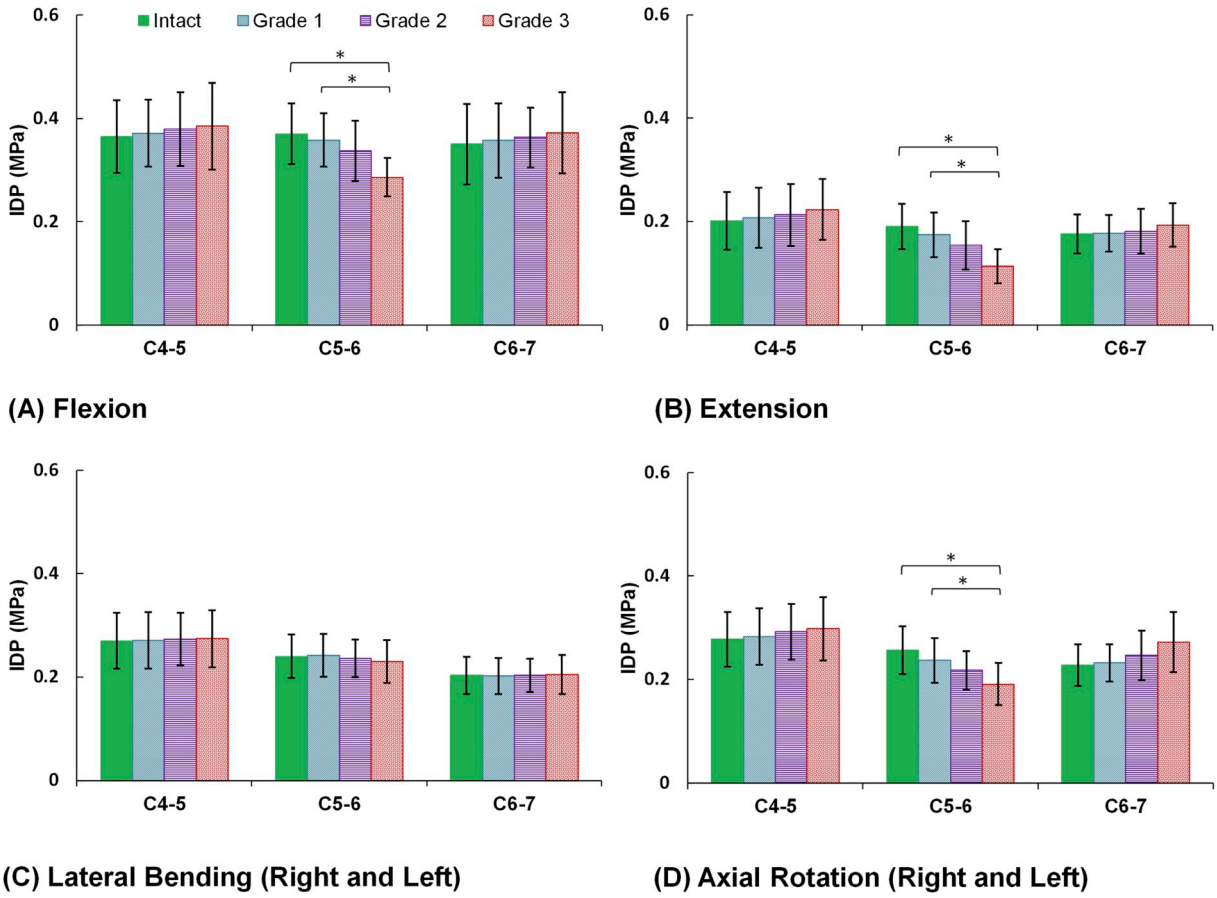

Fig. 8. Variation of the intradiscal pressure in C4-C5, C5-C6, and C6-C7 levels in simulated Intact and altered cervical spine (Grade 1 to 3). The error bars indicate the standard deviation and p value less than 0.05 was considered as significant difference and marked by "*".

percentage of difference was less than 15% (Fig. 6). Table 3 depicts the comparison between the exact and parametric models for the same geometry. Similar trends can be observed for the ROM, IDP, and fiber strain, while the FJF and maximum stress in the AF ground were slightly increased in parametric modeling (Table 3).

To evaluate the model's clinical application in patients with disc degenerative disease (DDD), the inter-segmental ROM at the C5-C6 level and adjacent levels (i.e., C3-C4 and C6-C7) in the DDD cervical spine models (Grades 1 to 3) were compared with the ROM in the model with intact discs (Fig. 7). The results indicate that the ROM demonstrated no changes upon simulation of grade 1 and grade 2 disc degeneration (Fig. 7). On the other hand, Grade 3 showed a significant decrease in the ROM in flexion, extension, as well as axial rotation (Fig. 7). The ROM slightly increased for the adjacent levels in flexion, extension, and axial rotation, but it was not statistically significant. The same trend was observed for the IDP in C5-C6 and adjacent levels (Fig. 8). Maximum Von-Mises stress in the AF significantly increased for models with Grade 3 in flexion, extension, as well as axial rotation (Fig. 9). The FJF increased for both C5-C6 and adjacent levels in extension and axial rotation (Fig. 10).

4. Discussion

The main contribution of this study was the development and validation of a simplified, geometrically-personalized lower cervical spine model with automatic update features and clinically driven, user-friendly interface. The logistic feasibility and applicability of the model in clinical settings were demonstrated by simulating 3 grades of cervical spine degeneration/alteration using 6 individual FE models in order to quantitatively evaluate the effects of the various degrees of disc alteration on the motion patterns, IDP, and maximum stress in the AF and FJF.

The results of the current parametric model were overall in good agreement with our previous FE exact geometry model [23]. However, higher FJF values in the parametric model suggest that simplification of the geometry of the facet joints, in particular, may alter the predicted force (approximately by less than 33%) in different directions. However, simplification of the facet joint geometry was common in some previous cervical and lumbar FE models [31,49]. Furthermore, using the same geometry, both parametric and exact models were in good agreement with in-vitro experimental data found in literature [9]. On the other hand, it is important to emphasize that the calculation time decreased from 18 h using the exact model to 17 min using the current parametric model. The exact modeling effort involved the extraction of complex geometry from CT scanned images using image processing software (i.e., MIMCS) and exporting them to FE software, a quite tedious and time-consuming procedure, rendering the logistics quite challenging in clinical settings. Alternatively, the parameters defined in the current parametric model can be extracted by users from AP and Lateral X-ray images in less than 5 min and easily input to the FE software, as shown by our clinical collaborators.

The calculated motion patterns for 6 individual subjects (Fig. 5) reveal wide variability, confirming the influence of geometry on the biomechanical response of the lower cervical spine. This is typically neglected in current exact FE models, which continue to use one or few averaged anatomical parameters. From a clinical perspective, a robust,

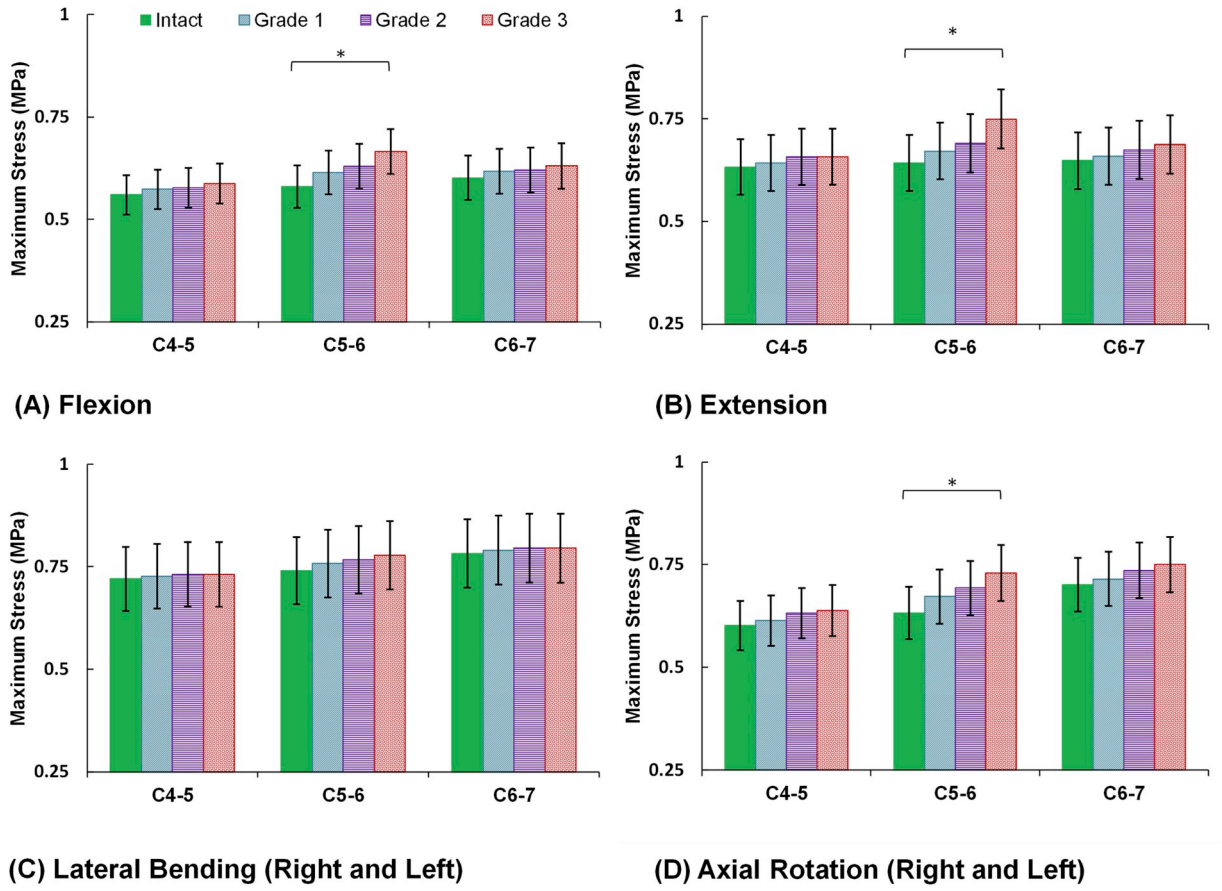

Fig. 9. Variation of the maximum stress in annulus fibrosus ground in C4-C5, C5-C6, and C6-C7 levels in simulated Intact and altered cervical spine (Grade 1 to 3). The error bars indicate the standard deviation and p value less than 0.05 was considered as significant difference and marked by "*".

time-effective parametric model, which incorporates patient-specific geometry, would be invaluable for devising appropriate treatment/surgical planning strategies. The clinical simulation revealed that severe disc alteration (i.e., grade 3) significantly affects the ROM of the altered disc in flexion, extension and axial rotation, while slightly affecting adjacent levels. The same trend was observed for the IDP on the C5-C6 intervertebral disc and adjacent levels (i.e., C4-C5 and C6-C7). This is in alignment with literature where decreased ROMs in altered and adjacent discs were reported in the elderly [50], as well as in previous exact FE studies [51]. In addition, disc alteration increased the maximum stress in both in the AF and the FJF for C5-C6 and adjacent level, also in alignment with previous reports in literature [51].

The simplicity inherent to parametric models allows for fast automatic mesh generation, and yet one needs to keep in mind that the geometry of the current parametric model was built based on simple shapes, such as circles, rectangles, and ellipses and that the model is symmetric. Furthermore, although comparison of the current model with previous exact models, including ours, demonstrates similar trends in terms of the ROM, IDP, FJF, and stress distribution, certain parameters, such as the stress distribution contours, can be evaluated more precisely in exact modeling, which may or may not be of interest in certain clinical evaluations. The material properties of the current FE model remain constant for different individuals, which is a clear limitation, in terms of clinically-driven patient-specific model. However, there are no current guidelines in literature on how to differentiate the exact material properties for different spinal components. Determination of the material properties of various cervical spine components in both healthy and pathological conditions, based on individualized experimental data, is important towards developing more clinically-applicable patient-specific models [52]. As the objective of this work was to develop and validate a methodology for more effective use of FE modeling in clinical settings, the variation in mechanical properties was neglected as it is difficult to be measured in clinics, but it remains a framework for future sensitivity analyses to enhance the model. In this study, we also neglected the effects of active muscle forces. The current osseo-ligamentous FE model is designed for static clinical settings, and as such can compensate for the global response of the lower cervical spine model for patients. To add patient-specific muscle forces, an additional inverse dynamics algorithm should be coupled with the current FE model. Future investigations may benefit by entertaining this.

In summary, this study presents a novel validated subject-specific FEM as a potential valuable tool for noninvasive, time and cost effective analyses of cervical spine biomechanical (kinematic and kinetic) changes associated with various injury/disease, which can be used for informed clinical decision-making. Our preliminary results demonstrate that the current model could provide surgeons with quantitative data that may be valuable for better treatment and surgical planning towards enhanced clinical outcomes.

Conflict of interest

The authors declare that the research was conducted in the absence of any commercial or financial relationships that could be construed as a potential conflict of interest.

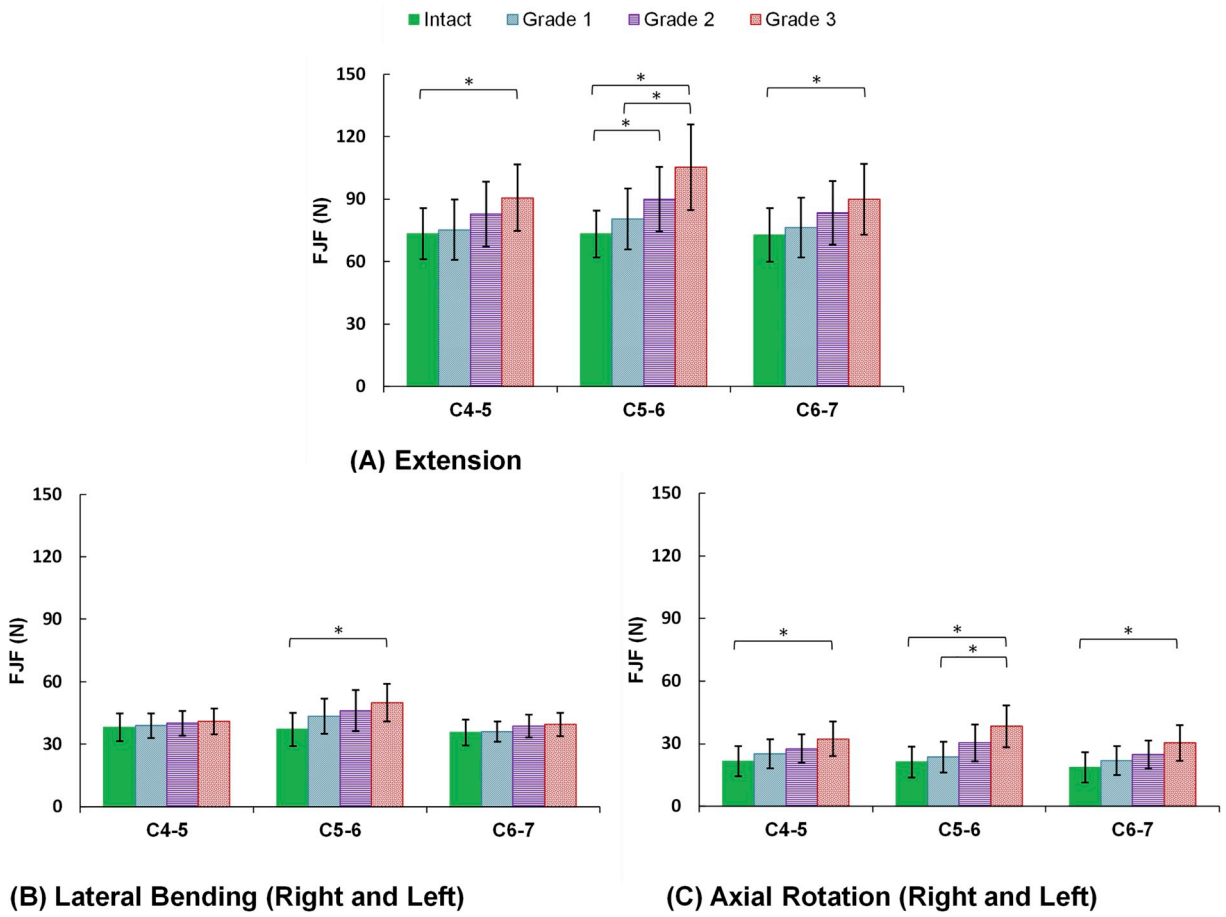

Fig. 10. Variation of the facet joint forces in C4-C5, C5-C6, and C6-C7 levels in simulated Intact and altered cervical spine (Grade 1 to 3). The error bars indicate the standard deviation and p value less than 0.05 was considered as significant difference and marked by "*".

References

[1] M. Nordin DirSci, V.H. Frankel, Basic Biomechanics of the Musculoskeletal System, 4 ed., Lippincott Williams & Wilkins Healt, 2012.

[2] D. Eddy, J. Congeni, K. Loud, A review of spine injuries and return to play, Clin. J. Sport Med. 15 (2005) 453–458.

[3] Y. Yu, H. Mao, J.S. Li, et al., Ranges of cervical intervertebral disc deformation during an in vivo dynamic flexion-extension of the neck, J. Biomech. Eng. 139 (2017).

[4] W.J. Anderst, W.F. Donaldson 3rd, J.Y. Lee, J.D. Kang, Continuous cervical spine kinematics during in vivo dynamic flexion-extension, Spine J. 14 (2014) 1221–1227.

[5] C. Dehner, S. Schick, W. Hell, P. Richter, M. Kraus, M. Kramer, In-vivo kinematics of the cervical spine in frontal sled tests, Glob. J. Health Sci. 5 (2013) 115–126.

[6] A.L. Clavenna, W.J. Beutler, M. Gudipally, M. Moldavsky, S. Khalil, The biomechanical stability of a novel spacer with integrated plate in contiguous two-level and three-level ACDF models: an in vitro cadaveric study, Spine J. 12 (2012) 157–163.

[7] T. Miura, M.M. Panjabi, P.A. Cripton, A method to simulate in vivo cervical spine kinematics using in vitro compressive preload, Spine 27 (2002) 43–48.

[8] L.P. Wu, Y.K. Li, B.J. Liang, D. Manas, J.H. Fan, Morphological changes of the in vitro cervical vertebral canal and its cast form during flexion, extension, and lateral bending, J. Manip. Physiol. Ther. 33 (2010) 132–137.

[9] M.M. Panjabi, J.J. Crisco, A. Vasavada, et al., Mechanical properties of the human cervical spine as shown by three-dimensional load–displacement curves, Spine 26 (2001) 2692–2700.

[10] S. Kumaresan, N. Yoganandan, F.A. Pintar, D.J. Maiman, Finite element modeling of the cervical spine: role of intervertebral disc under axial and eccentric loads, Med. Eng. Phys. 21 (1999) 689–700.

[11] N. Yoganandan, S.C. Kumaresan, L. Voo, F.A. Pintar, S.J. Larson, Finite element modeling of the C4–C6 cervical spine unit, Med. Eng. Phys. 18 (1996) 569–574.

[12] H.-W. Ng, E.-C. Teo, Nonlinear finite-element analysis of the lower cervical spine (C4–C6) under axial loading, J. Spinal Disord. 14 (2001) 201–210.

[13] A. Musapoor, M. Nikkhoo, M. Haghpanahi, A finite element study on intra-operative corrective forces and evaluation of screw density in scoliosis surgeries, Proc. Inst. Mech. Eng. H 232 (2018) 1245–1254.

[14] N. Kallemeyn, A. Gandhi, S. Kode, K. Shivanna, J. Smucker, N. Grosland, Validation of a C2–C7 cervical spine finite element model using specimen-specific flexibility data, Med. Eng. Phys. 32 (2010) 482–489.

[15] H. Schmidt, F. Galbusera, A. Rohlmann, A. Shirazi-Adl, What have we learned from finite element model studies of lumbar intervertebral discs in the past four decades? J. Biomech. 46 (2013) 2342–2355.

[16] M. Nikkhoo, Y.-C. Hsu, M. Haghpanahi, M. Parnianpour, J.-L. Wang, A meta-model analysis of a finite element simulation for defining poroelastic properties of intervertebral discs, Proc. IME H J. Eng. Med. 227 (2013) 672–682.

[17] M. Dreischarf, T. Zander, A. Shirazi-Adl, et al., Comparison of eight published static finite element models of the intact lumbar spine: predictive power of models improves when combined together, J. Biomech. 47 (2014) 1757–1766.

[18] M.M. Panjabi, The stabilizing system of the spine. Part II. Neutral zone and instability hypothesis, J. Spinal Disord. 5 (1992) 390–397.

[19] M.M. Panjabi, The stabilizing system of the spine. Part I. Function, dysfunction, adaptation, and enhancement, Clin. Spine Surg. 5 (1992) 383–389.

[20] A. Rohlmann, T. Zander, M. Rao, G. Bergmann, Applying a follower load delivers realistic results for simulating standing, J. Biomech. 42 (2009) 1520–1526.

[21] A. Jalalian, I. Gibson, E.H. Tay, Computational biomechanical modeling of scoliotic spine: challenges and opportunities, Spine Deform. 1 (2013) 401–411.

[22] H. Schmidt, A. Shirazi-Adl, F. Galbusera, H.J. Wilke, Response analysis of the lumbar spine during regular daily activities–a finite element analysis, J. Biomech. 43 (2010) 1849–1856.

[23] M. Nikkhoo, A. Tahassory, M. Haghpanahi, Design and biomechanical study of the first Iranian cervical cage using finite element analyses, Iran. J. Biomed. Eng. 8 (2014) 203–212.

[24] C. Wong, P.M. Gehrchen, T. Darvann, T. Kiaer, Nonlinear finite-element analysis and biomechanical evaluation of the lumbar spine, IEEE Trans. Med. Imaging 22 (2003) 742–746.

[25] K. Wang, Z. Deng, H. Wang, Z. Li, H. Zhan, W. Niu, Influence of variations in stiffness of cervical ligaments on C5-C6 segment, J. Mech. Behav. Biomed. Mater. 72 (2017) 129–137.

[26] Z. Deng, K. Wang, H. Wang, T. Lan, H. Zhan, W. Niu, A finite element study of traditional Chinese cervical manipulation, Eur. Spine J. 26 (2017) 2308–2317.

[27] M.E. Kunkel, H. Schmidt, H.J. Wilke, Prediction equations for human thoracic and lumbar vertebral morphometry, J. Anat. 216 (2010) 320–328.

[28] K. Khalaf, M. Nikkhoo, M. El-Rich, et al., Development of a parametric subject-specific finite element model to investigate the lumbar spine response before and after one-level posterior fusion, 8th World Congress of Biomechanics, Oxford

Abstracts Ltd, Dublin, Ireland, 2018.
[29] K. Khalaf, M. Nikkhoo, M. Parnianpour, M. Bahrami, C.-H. Cheng, Development of A parametric subject-specific finite element modelof the lower cervical spine to evaluate the effect of disease on the motion patterns, Orthop. Proc. 100-B (2018) 88.
[30] J.P. Little, H. De Visser, M.J. Pearcy, C.J. Adam, Are coupled rotations in the lumbar spine largely due to the osseo-ligamentous anatomy?—a modeling study, Comput. Methods Biomech. Biomed. Eng. 11 (2008) 95–103.
[31] A. Laville, S. Laporte, W. Skalli, Parametric and subject-specific finite element modelling of the lower cervical spine. Influence of geometrical parameters on the motion patterns, J. Biomech. 42 (2009) 1409–1415.
[32] A. Calvo-Echenique, J. Cegonino, R. Chueca, A. Perez-Del Palomar, Stand-alone lumbar cage subsidence: a biomechanical sensitivity study of cage design and placement, Comput. Methods Progr. Biomed. 162 (2018) 211–219.
[33] M. Nikkhoo, M. Haghpanahi, M. Parnianpour, J.-L. Wang, Dynamic responses of intervertebral disc during static creep and dynamic cyclic loading: a parametric poroelastic finite element analysis, Biomed. Eng.: Appl. Basis Commun. 25 (2013) 1350013.
[34] F. Niemeyer, H.J. Wilke, H. Schmidt, Geometry strongly influences the response of numerical models of the lumbar spine–a probabilistic finite element analysis, J. Biomech. 45 (2012) 1414–1423.
[35] B.D. Stemper, N. Yoganandan, F.A. Pintar, Effects of abnormal posture on capsular ligament elongations in a computational model subjected to whiplash loading, J. Biomech. 38 (2005) 1313–1323.
[36] X. Zhao, L. Du, Y. Xie, J. Zhao, Effect of lumbar lordosis on the adjacent segment in transforaminal lumbar interbody fusion: a finite element analysis, World Neurosurg. 114 (2018) e114–e120.
[37] A. Chien, D.M. Lai, S.F. Wang, W.L. Hsu, C.H. Cheng, J.L. Wang, Comparison of cervical kinematics, pain, and functional disability between single- and two-level anterior cervical discectomy and fusion, Spine 41 (2016) E915–E922.
[38] N. Yoganandan, S. Kumaresan, F.A. Pintar, Geometric and mechanical properties of human cervical spine ligaments, J. Biomech. Eng. 122 (2000) 623.
[39] J.A. Wheeldon, B.D. Stemper, N. Yoganandan, F.A. Pintar, Validation of a finite element model of the young normal lower cervical spine, Ann. Biomed. Eng. 36 (2008) 1458–1469.
[40] H. Schmidt, F. Heuer, U. Simon, et al., Application of a new calibration method for a three-dimensional finite element model of a human lumbar annulus fibrosus, Clin. Biomech. 21 (2006) 337–344.
[41] N. Toosizadeh, M. Haghpanahi, Generating a finite element model of the cervical spine: estimating muscle forces and internal loads, Sci. Iran. 18 (2011) 1237–1245.
[42] H. Schmidt, F. Heuer, J. Drumm, Z. Klezl, L. Claes, H.J. Wilke, Application of a calibration method provides more realistic results for a finite element model of a lumbar spinal segment, Clin. Biomech. 22 (2007) 377–384.
[43] I. Ziv, C. Maroudas, G. Robin, A. Maroudas, Human facet cartilage: swelling and some physicochemical characteristics as a function of age, Spine 18 (1993) 136–146.
[44] E. Okada, M. Matsumoto, H. Fujiwara, Y. Toyama, Disc degeneration of cervical spine on MRI in patients with lumbar disc herniation: comparison study with asymptomatic volunteers, Eur. Spine J. 20 (2011) 585–591.
[45] A. Suzuki, M.D. Daubs, T. Hayashi, et al., Magnetic resonance classification system of cervical intervertebral disk degeneration: its validity and meaning, Clin. Spine Surg. 30 (2017) E547–E553.
[46] H. Schmidt, A. Kettler, A. Rohlmann, L. Claes, H.J. Wilke, The risk of disc prolapses with complex loading in different degrees of disc degeneration - a finite element analysis, Clin. Biomech. 22 (2007) 988–998.
[47] Q.H. Zhang, E.C. Teo, H.W. Ng, V.S. Lee, Finite element analysis of moment-rotation relationships for human cervical spine, J. Biomech. 39 (2006) 189–193.
[48] V.K. Goel, J.D. Clausen, Prediction of load sharing among spinal components of a C5-C6 motion segment using the finite element approach, Spine 23 (1998) 684–691.
[49] J.-L. Wang, M. Parnianpour, A. Shirazi-Adl, A.E. Engin, Viscoelastic finite-element analysis of a lumbar motion segment in combined compression and sagittal flexion, Spine 25 (2000) 310–318.
[50] K.A. Kuhlman, Cervical range of motion in the elderly, Arch. Phys. Med. Rehabil. 74 (1993) 1071–1079.
[51] W.M. Park, K. Kim, Y.H. Kim, Changes in range of motion, intradiscal pressure, and facet joint force after intervertebral disc and facet joint degeneration in the cervical spine, J. Mech. Sci. Technol. 29 (2015) 3031–3038.
[52] Y.H. Kim, B. Khuyagbaatar, K. Kim, Recent advances in finite element modeling of the human cervical spine, J. Mech. Sci. Technol. 32 (2018) 1–10.